Quantification of the Dynamic-stall Model Uncertainty in the Performance Prediction of Vertical Axis Wind Turbines

Journal of Physics: Conference Series **1618** (2020) 052071 doi:10.1088/1742-6596/1618/5/052071

Quantification of the Dynamic-stall Model Uncertainty in the Performance Prediction of Vertical Axis Wind Turbines

Giacomo Persico, Andrea G. Sanvito, Vincenzo Dossena

Laboratory of Fluid-Machines, Dipartimento di Energia, Politecnico di Milano, Via Lambruschini 4, 20156 Milano, Italy

E-mail: giacomo.persico@polimi.it

Abstract. Low-fidelity predictions for vertical-axis wind turbines are affected by uncertainty due to the complexity of the rotor aerodynamics. In particular, in the most common operating conditions the blades undergo periodic excursions beyond the static stall limit, activating dynamic-stall effects. In this study we show how advanced dynamic-stall models, implemented in the frame of the Blade-Element-Momentum theory, are able to upgrade significantly the prediction of low-fidelity tools, both in deterministic and probabilistic terms. In particular, an uncertainty quantification is performed to investigate the epistemic uncertainty of the Strickland dynamic-stall model, introducing a large variability on the empirical parameters appearing in the formulation. The resulting variability in the power coefficient and torque exchange, compared to corresponding wind-tunnel and high-fidelity CFD values, remains relatively limited and, in the conditions around peak efficiency, it is comparable with the measurement uncertainty of the experiment. As a further relevant conclusion, the model uncertainty does not alter the general outcome of the deterministic model, thus demonstrating the robustness of the DMST predictions obtained in the present study.

1. Introduction

Wind energy has experienced a stable growth in the last 20 years, reaching a total installed power of 591 GW in 2018, according to the Global Wind Energy Council. Nevertheless, the share of electricity production harvested from wind is still relatively low (5.6% in 2017) with respect to the forecasts for the next decade (European Countries, for example, have set a target of 30% of electricity produced by renewable energy sources in 2030). This drives the research on wind energy technology towards more efficient and reliable conversion systems as well as towards novel/alternative conversion systems that might be competitive with the leading horizontal-axis wind turbine technology in specific applications, for whose this latter exhibits limitations and efficiency reduction. In this context, a new interest has recently arisen in the lift-driven Vertical-Axis Wind Turbine (VAWT) because of its several inherent advantages (omni-directionality, low tip speed ratio, generator at the bottom) that make it attractive for both small scale urban applications and large-scale floating off-shore installations. However, the complex and unsteady aerodynamics of the VAWT introduces significant uncertainties in the rotor design, which ultimately penalize the turbine aerodynamic efficiency and mechanical integrity with respect to the widespread horizontal-axis configuration.

The aerodynamic design of wind turbines mostly relies on 'low-fidelity' engineering approaches; even though high-fidelity Computational Fluid Dynamics (CFD) tools have been successfully applied to VAWTs [1, 2, 3, 4], they are mainly applied for analyzing existing configurations and not routinely used for design, due to the severe computational cost of each of those simulations. The engineering approach based on the Blade Element Momentum (BEM) theory, and reformulated as the Double Multiple Stream-Tube (DMST) method by Paraschivoiu [5] for VAWTs, allows efficient design procedures and have been proven to provide accurate performance estimates against experiments for VAWTs [6, 7]. However, such an approach has to rely on airfoil polars in a very wide range of angle of attack, well beyond the static-stall and deep-stall limit, and on several empirical or semi-empirical corrections, resulting inevitably affected by uncertainty in the input correlations.

In such a context, the systematic Uncertainty Quantification (UQ) in low-fidelity predictions of VAWT performance is crucial to evaluate the degree of reliability of the designed configurations. In recent years, thanks to the progresses in the computational science and capability, novel techniques have been developed and successfully applied to determine the propagation of uncertainty from the inputs to the outputs of non-linear solvers [8], combining the Monte-Carlo method with different classes of surrogates, based on gaussian processes [9] or polynomial chaos expansions [10].

The dynamic stall is one of the most significant sources of uncertainty affecting VAWT design, due to the inherent unsteadiness and non-linearity of the process. This is especially valid for engineering methods, in which the effects of dynamic stall have to be introduced in an over-simplified way. Even though several models were proposed in Literature (Gormont [11], Strickland [12], Leishmann and Beddoes [13], Sheng [14]), a systematic evaluation of the associated uncertainty on VAWT performance prediction is not straightforward and, to the authors' best knowledge, it is still not available in Literature. In the present work, we obtain performance estimates for a small-scale VAWT applying an in-house DMST code, and we analyze the sensitivity of the predicted performances to the uncertainty of the dynamic-stall model by resorting to a systematic UQ analysis. In this work we investigate the impact of the model proposed by Strickland and collaborators [12], based on the empirical synthesis of unsteady aerodynamic experimental data. Since the model relies on several coefficients, we investigate the epistemic uncertainty deriving from the uncertain quantitative values of all the aforementioned coefficients, without altering the functional form of the model itself.

The results of the DMST are validated against experimental benchmark data obtained through dedicated wind-tunnel measurements at Politecnico di Milano [15, 16], and also by resorting to two-dimensional CFD simulation of the turbine on the midspan section. Experiments include power coefficient (C_p) measurements at different tip-speed ratios (TSR) and phase-resolved shaft torque measurements at $TSR = 2.4$. The experimental uncertainty is directly compared with the one resulting from the DMST calculation.

2. VAWT layout and performance parameters

This study focuses on a small-scale VAWT for distributed micro-generation (peak power of about 200 W). The rotor features a straight H-shape and it is composed by three un-staggered NACA0021 blades whose length is 1.46 m and whose profile chord is 0.086 m; the rotor diameter is 1.03 m (the resulting swept area is of about 1.5 m^2). Figure 1 shows the design of the rotor, including the two symmetric systems of struts, above and below the rotor equatorial plane; the struts are composed by radially flat elements. Full details on the turbine geometrical features as well as on the turbine operating and performance parameters can be found in [15].

The VAWT model was studied experimentally in three test-campaigns performed in the large-scale wind tunnel of the Politecnico di Milano (Italy); the test section is characterized by a square cross-section of about 16 m^2 and it is 6-meter long; the flow velocity can range between 0 and

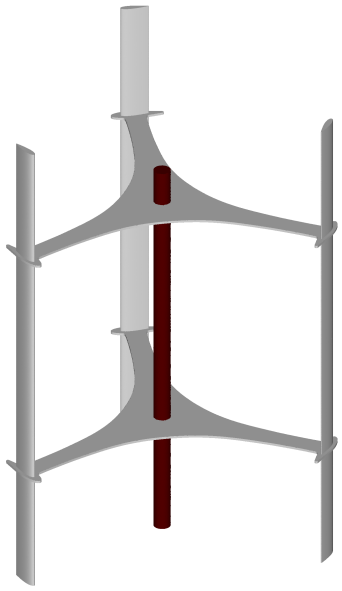

Figure 1. VAWT geometric layout.

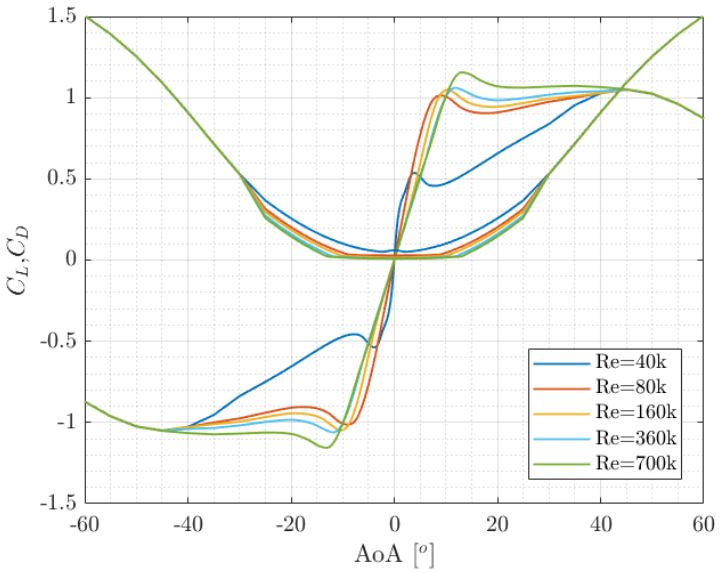

Figure 2. Lift and drag coefficients for airfoil NACA0021 for different Reynolds number.

50 m/s, with inlet turbulence intensity below 1%. The experimental benchmark data used as reference in this work were obtained in free-jet conditions, i.e. removing the wind-tunnel walls around the turbine, which allowed reducing the wind-tunnel blockage factor below 1.5% [17].

The test campaign focused on performance, thrust and velocity measurements in the turbine wake [15]. Performance data were measured by combining angular speed measurements, obtained by an absolute encoder, with torque measurements, obtained by a precision torque meter. An evaluation of the measurement uncertainty on the power coefficient measurement was performed by applying the classical theory of Uncertainty Propagation, obtaining different uncertainty ranges at varying TSR. In the following analysis, each experimental datum will appear in the plots with an error bar representing the estimated experimental uncertainty.

3. The Double-Multiple Stream Tube Code

An in-house Blade Element Momentum tool relying on the Double Multiple Stream Tube (DMST) approach has been developed and applied to assess the performance of the small scale H-shaped VAWT described above and compared with experimental results. This section reports the details of the implementation and a deterministic comparison with the experiments, to highlight the general predictive capability of the code. Even though the DMST approach is nowadays consolidated in Literature, a presentation of the detailed modeling aspects of the code is deemed necessary as foundation for the uncertainty analysis reported in the next section.

The DMST code developed in this work applies the steady-state formulation of the blade-element momentum theory for double multiple stream-tubes, considering the upwind and downwind sections of the rotor, and it encompasses several corrections to attain more accuracy in the performance predictions. At first, the overall code concept is presented, then the sub-models are discussed, with a special focus on the dynamic-stall models implemented.

3.1. Basic code layout

The availability of accurate input polar data is crucial to achieve reliable predictions with low-fidelity codes, as shown by Bianchini et al. [18]. In this work airfoil polars of the symmetric

profile NACA0021 are used to obtain lift and drag coefficients within a range of angle of attack from -180^o to $+180^o$ and a range of Reynolds number comprised between $40'000$ and $5'000'000$, so to cover all the possible turbine operating conditions. The lift and drag coefficient polars actually used in this study are shown in Figure 2. Polars were built by combining three methods: (i) the XFOIL tool, which uses the panel method combined with an integral boundary layer solution (Ncrit=9 is assumed for the free transition model), in the region of attached flow up to the static stall; (ii) the Viterna correction [19] in the post-stall region, in order to have a smoother transition of aerodynamic coefficients between the linear and deep-stall regions; (iii) the semi-empirical correlation reported in [20] from deep-stall angle onwards, where leading edge flow separation takes place.

The DMST code treats each stream tube as independent implying variable axial induction factor a as proposed by Paraschivoiu in [5]. The numerical model envisages the division of each actuator disk, either the upwind and the downwind one, in N stream tubes assigning a constant step in azimuthal angle $d\theta_i$. After a sensitivity analysis ensuring convergence of the solution, $N = 40$ was chosen. Since the induction factor is directly linked to the velocity triangles an iterative procedure is performed. Foremost, an initial value is guessed and kinematic quantities are calculated for each TSR (varying wind speed V_0) for $i-th$ stream tube considered, according to the following expressions:

$$V_{D1,i} = (1 - a_{D1,i})\, V_0 \tag{1}$$

$$W_{rel,i} = \sqrt{((V_{D1,i}\, cos\theta_i + \Omega R)\, cos\gamma_c)^2 + (V_{D1,i}\, sin\theta_i\, cos\delta_c)^2} \tag{2}$$

$$\alpha_i = \arctan\left(\frac{V_{D1,i}\, sin\theta_i\, cos\delta_c}{(V_{D1,i}\, cos\theta_i + \Omega R)\, cos\gamma_c}\right) \tag{3}$$

where $V_{D1,i}$ is wind velocity approaching upwind actuator disk, $W_{rel,i}$ is the relative velocity experienced by the blade and α_i is the angle of attack. The code was conceived for being suitable to general swirling (angle γ_c) and curved (angle δ_c) rotor layouts; however, since in this study we focus on a straight H-shaped VAWT, $\gamma_c = 0$ and $\delta_c = 0$. Interpolating values of the polars, aerodynamic coefficients are known and thrust coefficient is calculated from tangential and normal force coefficients. Hence, a new value of induction factor is attained via Glauert correction to model the turbine in turbulent wake state (in particular the Burton correlation have been implemented, as documented in [21]). The same procedure is followed for the downwind stream tubes, assuming as upcoming wind speed the far-wake velocity of the upstream stream-tube $V_{D2,i} = (1 - 2a_{D1,i})\, V_{0,i}$.

By iterating on the thrust coefficient until convergence (with tolerance set to 10^{-4}), the distribution of induction factor, aerodynamic forces, and torque over the turbine revolution are eventually obtained, from that the overall power and power coefficient C_p are calculated.

$$P = N_b \frac{1}{2\pi}\left(\int_0^{\pi} \Omega T_i^{D1}\, d\theta_i + \int_{\pi}^{2\pi} \Omega T_i^{D2}\, d\theta_i\right) \tag{4}$$

$$C_P = \frac{P}{\frac{1}{2}\rho V_0^3 H D} \tag{5}$$

3.2. High-order corrections

The accuracy of DMST codes is known to highly benefit from the introduction of high-order corrections. The following corrections are implemented in the present work: flow curvature effect, finite aspect ratio correction, strut parasitic torque, alongside the dynamic-stall model, which is the core of this study and it is treated in a dedicated subsection.

Due to their inherent motion, VAWT blades move along curvilinear trajectories, while aerodynamic polar data are obtained in straight flows; this involves an altered boundary layer, caused by the centrifugal force, and the airfoil mean line not corresponding to the tangent line; as a result, the flow conditions (relative velocity and angle of attack) perceived by the airfoil change along the chord. In the code this so-called curvature effect is taken into account using the Goude's correlation [22], which alters the angle of attack during the blade revolution to mimic the effect of effects of flow curvature. In this particular work, the corrected angle of attack is employed to evaluate the aerodynamic coefficients only, while the physical angle of attack remains unaltered as well as the directions along which the lift and drag forces act.

As a second correction, the two-dimensional flow assumption of the basic DMST is not representative of the complex fluid dynamics of a VAWT, since the finite blade length implies a reduction of angle of attack caused by the spanwise pressure gradient towards the tip of the blades. According to Prandtl-Lanchester theory, the effect can be considered by proper adjustment of the lift and drag coefficients. Introducing this correction, VAWT performance decreases due to the combination of a reduced angle of attack (which lowers the lift) and of the induced drag.

Flow-curvature and aspect-ratio corrections are the two basilar sub-models implemented in common DMST codes; therefore, it is interesting to evaluate the predictive capability of the present code including these two corrections only. Figure 3 compares the experimental data taken from [15] with DMST predictions in terms of turbine power coefficient, over the entire operating range of the machine, by varying the oncoming wind speed in the range 6-16 m/s at a constant angular speed of 400 rpm (as done in wind-tunnel experiments). The trend of power coefficient matches well with the experimental one even though, especially for TSR higher than that of peak efficiency (TSR = 2.7), the computed curve diverges significantly from the measured one due to an evident over-prediction of the power harvested by the machine.

These observations indicate that a further modeling effort is required to improve DMST prediction. Three-dimensional corrections, in particular, are especially relevant for the present turbine, due to the wide and flat struts, which are expected to induce a significant passive torque. As shown by the 2.5D and 3D simulations reported in [4], the strut effect plays the major role at high TSR, for that the present prediction exhibits the largest differences with the experiments. The parasitic torque of the struts is evaluated after convergence is reached for each stream-tube, and it is then subtracted from the overall torque of the machine. The struts are modeled as flat plates with variable chord along the radius. The drag coefficient is independent to Reynolds number and assumed constant. The model here used follows the one described in detail and applied in Bianchini et al., 2019 [6], based on the evaluation of the velocity for each stream tube along the strut radius

By introducing the strut parasitic torque into the model, the values of predicted power coefficient reduce over the entire curve as shown in Figure 3. As expected, the passive torque due to struts play a key role at high TSR, but it has a significant effect also for TSRs around peak efficiency, leading however to a slight but visible under-prediction of power coefficient in the operating range of highest importance, i.e. the one close to peak power coefficient. However, the correction for dynamic stall model is still to be considered, and its implementation and impact on the mean turbine performance is discussed in the next section.

3.3. Dynamic stall model

Dynamic stall occurs when the blade is subjected to a rapid variation of angle of attack, so that the airfoil undergoes periodic excursions in the post-stall region. The airfoil pressure distribution cannot vary instantaneously and the effect is that lift and drag curves are modified with respect to static 2D data, exhibiting an hysteretic behaviour. Such effects occur in most VAWT operating conditions: due the high variation of angle of attack, especially al low TSR,

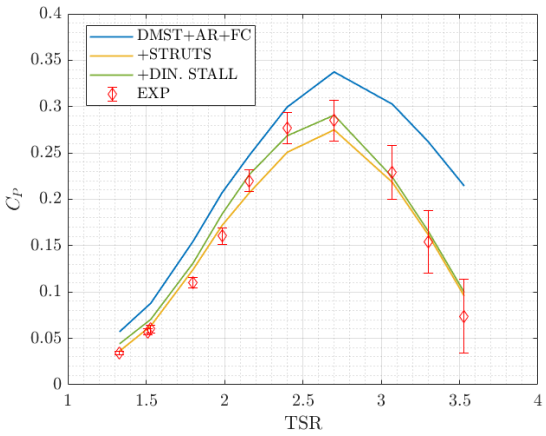

Figure 3. Power coefficient curve prediction for different sub-models against experiments.

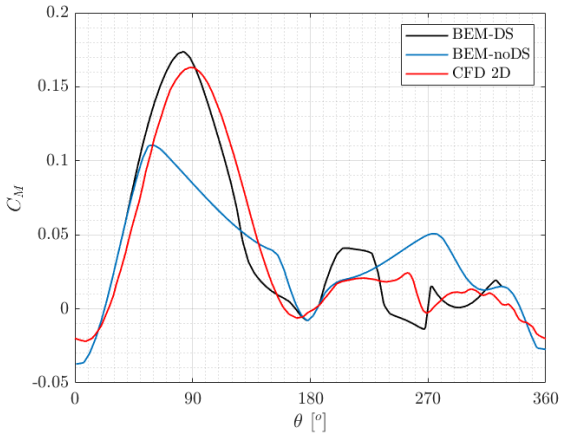

Figure 4. Torque exchanged by the rotor along the revolution for TSR = 2.4 for different sub-models against experiments.

the angle of attack may periodically overcome the static stall threshold. Literature consists of several dynamic stall models, the first one being proposed by Gormont [11], based on reference angle correction to which static polars are referred; extensions and adaptations of this early model were proposed by Strickland [12] and Paraschivoiu [5] specifically for VAWTs. Alternative to such models, Leishmann and Beddoes developed a physical-based formulation to account for unsteady aerodynamics as well as leading and trailing edge flow separation, recently adapted by Sheng [14] for VAWTs. Each of the above said models are implemented in DMST code; nonetheless, the present study is focused on a single dynamic stall model in presence of uncertain parameters. In particular, the Strickland's model was chosen, since, in the present implementation, it guaranteed the best agreement with the available experimental results in deterministic terms (in fact, the authors developed an alternative time-marching BEM code to couple the DMST with the Leishmann-Beddoes model, however they faced difficulties in finding appropriate values for the parameters of the model in the range of Reynolds numbers of interest for this specific turbine).

The correction for the dynamic stall further increases the power coefficient prediction in the range of TSR around peak efficiency, while having a minimal impact at low and high TSR. Since the Strickland's model is activated as soon as AOAs are higher than the static stall limit, its contribution is detected from low TSR values, even though the quantitative effect of dynamic stall is limited for $TSR \leq 2$. The highest relevance of dynamic stall is actually found at medium TSR where the machine has its optimal operating condition. After that, the impact of dynamic stall reduces and finally vanishes from $TSR \geq 3.1$, as the peripheral speed becomes predominant with respect to wind speed and the angle of attack does not overcome the stall angles. The combination of all the sub-models ultimately results in an excellent agreement between the DMST prediction and the experimental data over the entire curve, so that all the predicted values lie within (or are slightly above, for $TSR \leq 2$) the uncertainty band of the experiment.

To proper investigate the action of the dynamic-stall model, the distribution of torque coefficient exchanged by one blade over the revolution is now investigated for a condition close to peak efficiency, namely TSR = 2.4. Figure 4 compares the DMST prediction obtained with and without the dynamic-stall model activated. The torque plot indicates that the dynamic stall delays the boundary layer separation and, hence, the subsequent decay of torque occurring

at 50^o visible in the trend obtained without the model implemented. As a result, the fraction of upwind stroke in the range $60^o \leq \theta \leq 120^o$ greatly benefits for the dynamic stall, which in this phase has a higher impact than the torque reduction in the downwind region. This explains the overall improvement of VAWT performance prediction when the dynamic stall is activated. However, the dynamic-stall alters significantly the torque exchange in the entire downwind half of the revolution. To better evaluate the physical significance of the model, it is interesting to complement the present analysis with a comparison with results achieved with a high-fidelity computational fluid-dynamic (CFD) simulation. CFD simulations were performed by applying a commercial code (Fluent) and by resorting to the general guidelines nowadays established for VAWT CFD simulations [23]. Two-dimensional calculations were performed to simulate the flow around the turbine in the equatorial section; the spatial and temporal resolutions were increased up to obtain a grid-independent solutions for a time-step corresponding to 0.2 deg and a mesh composed by 550000 cells. The standard $k - \omega$ SST turbulence model was used, with near-wall boundary layer resolution. High-resolution numerical schemes were used for the numerical integration of the equations (second-order upwind scheme for divergence terms and central differences for laplacian terms). Full details of the CFD simulations are reported in [24].

For TSR = 2.4, the CFD prediction provides a Cp = 0.27, which is in full agreement with both the corresponding experimental and DMST data (even though 3D effects are not included in the CFD simulation, their impact is deemed to be relatively limited for this condition, as indicated by the comparison among different models reported in Figure 3 and also by the similar comparative analysis reported in [6]). The computed torque coefficient, also reported in Figure 4, indicates a remarkable agreement with the DMST prediction obtained with the dynamic-stall model activated, thus indicating that the modeling effort required to implement the dynamic-stall model is crucial to obtain not just a good prediction of the overall turbine performance, but also to predict a more realistic instantaneous distribution of aerodynamic forcing on the blades, which is crucial for structural design.

In general, combination of experiments and CFD simulations suggest that very good deterministic results can be achieved with the present DMST code, suggesting however a relevant impact of the dynamic stall model at both mean and instantaneous level. The following section will investigate the effects of the Strickland model parameters to underline the dependence of the model to empirical constants, and their impact on VAWT predictions.

4. Uncertainty Quantification of Dynamic-Stall Model

In this section we propose an analysis of the epistemic uncertainty associated to the dynamic-stall model in the context of the DMST model described and assessed in the previous section. We will also investigate the impact of this uncertainty on the performance of the H-shaped VAWT described in Section 2. To do this in a systematic way, Uncertainty Quantification (UQ) techniques are used. UQ belongs to the general framework of probabilistic engineering and allows evaluating how the model uncertainty propagates throughout non-linear systems of equations, such as the complete DMST model. In addition to that, UQ techniques also allow to perform a sensitivity analysis to evaluate the relative impact of the input uncertainty on the quantity of interest [8].

4.1. UQ approach and implementation

The application of UQ techniques with non-intrusive approaches, i.e. without modifying the source code, requires the sampling of the deterministic model considering multiple realizations of the uncertain inputs; this is normally done by applying the Monte-Carlo Sampling (MCS) approach, considering a sufficient number of realizations within the Probability Density Function (PDF) of each uncertain variable, and all the combinations among them. Such an approach demands a very high number of simulations, of the order of 10^6, which makes it impracticable

if the cost of each simulation is - at least - of the order of a few minutes (which is the case of the present DMST code, to reconstruct the entire operational curve of the VAWT). However, alternative approaches exist, which complement the MCS with surrogate functions [9, 10] and efficient sampling techniques such as the Latin Hypercube Sampling (LHS). Such a strategy allows approximating the response of the system to the variability of the inputs with an analytical function, which is interpolated using a very a limited number of samples (of the order of 10^2-10^3). Then, the MCS is applied to the surrogate function only, so that each evaluation requires fractions of milliseconds. In this way, the computational cost of the UQ simulation for the present study is of the order of a couple of hours, for the entire operational curve of the machine.

In this study we use LHS for sampling and gaussian processes (or Kriging) combined with polynomial-chaos expansions (PCK) as surrogates. The UQ calculations were implemented within the *UQLab* framework [25]. This allowed obtaining analytical functional forms for the overall power coefficient and for the phase-resolved torque exchanged by both the rotor and single blades over a revolution. The MCS, applied to each of these quantities, allowed achieving the related probability distributions, statistical moments, and sensitivity indexes. In this way, an uncertainty band is evaluated for each one of the main outputs of the DMST.

4.2. UQ set-up

The unique source of uncertainty, in this work, is associated to the dynamic-stall model of Strickland. In particular, it provided a noteworthy improvement in the computational-experimental comparison in the range of TSR around peak efficiency, which is the most important operation range for a machine. Conversely, the dynamic-stall model caused a limited over-estimate of the turbine performance in the low TSR range, which is also important for the machine, especially in the start-up phase. This deterministic analysis indicates that the dynamic-stall model plays a crucial role in the turbine prediction, and justifies the interest in evaluating its associated uncertainty.

The functional form of the model was kept untouched, while the uncertainty was focused on the three empirical parameters that appear in the model, namely $K1$, γL and γD. They were originally obtained by synthesizing a wide set of experimental results reported in [11]. The model is indeed an adaptation of the original Gormond model, developed for helicopter applications, considering incompressible flows and symmetric airfoils as usually used in VAWTs. In particular, the factor K1 considers the asymmetry between the effects of negative variations of angle of attack, with respect to those observed for positive ones: an average observation of the Gormont's experiments [11] suggested indeed to halve the contribution of dynamic stall for negative variations of angle of attack. The two further coefficients appearing in the model are used to calculate the reference angle of attack that has to be used to correct the polar data in presence of dynamic stall, one for the lift coefficient (γL) and one for the drag one (γD).

For none of these parameters an experimental uncertainty band is available, so we opted for a conservative approach. Three multipliers were introduced in the model, one for each parameter, defined as f_{K1}, $f_{\gamma L}$, $f_{\gamma D}$. As usually done when the PDFs of the inputs are unknown, uniform PDFs were selected. The range of variability considered, also called the support of the PDF, was assigned as follows: for the coefficient f_{K1} the uncertainty range was defined from 0, i.e. no dynamic stall correction when the variability of angle of attack is in the negative range, and 2, i.e. to impose the same effects when the variability is in the positive or in the negative range; for the other two coefficients, the support was chosen in an exploratory way, considering variations of empirical parameter between the 50% and the 150% of the suggested range. The range of variability are reported in Table 1.

Table 1. Uncertain variable ranges for UQ on dynamic-stall model.

Input parameter	Range
f_{K1}	[0, 2]
$f_{\gamma L}$	[0.5,1.5]
$f_{\gamma D}$	[0.5,1.5]

4.3. UQ results

The UQ analysis was initialized considering multiple LHS applications, for different number of samples. The statistics of the quantities of interest, i.e. the power coefficient and the torque exchanged by the blade and by the rotor, were monitored until convergence was reached for a number of samples equal to 100.

On the basis of the LHS database, PCK models for the each quantity of interest were interpolated and sampled with a MCS technique so to obtain information on the statistical moments, in particular mean and standard deviation, and on the entire PDFs, in terms of support and distribution.

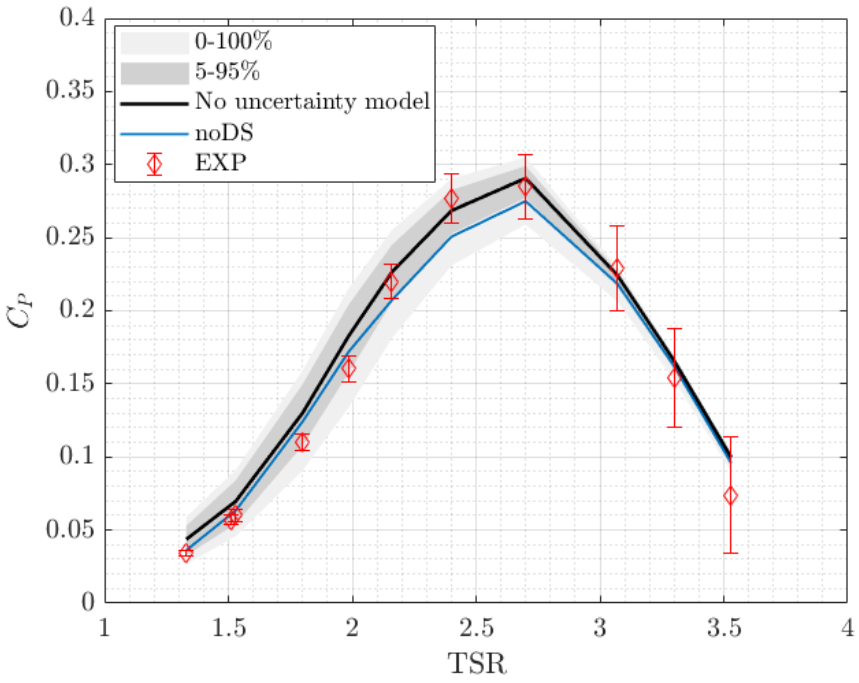

Figure 5. Power coefficient curve prediction with uncertainty bands against experiments.

The impact of uncertainty on the overall turbine performance is first considered, with reference to the curves reported in Figure 5. The figure reports the experimental data, with their 95% uncertainty bar, the deterministic curves for DMST with and without dynamic stall model, and two gray uncertainty bands, one considering a variability between the 5-th and then 95-th quantile, and one covering the entire support of the PDF. We first note that the variability vanishes for $TSR \geq 3.3$, where indeed the dynamic stall model never activates. Also, the uncertainty in the dynamic stall model generates a narrow variability at low TSR, which is

of the same order of the difference between the computed and the experimental data. Then, for $2 \leq TSR \leq 3.1$ the uncertainty bands of the experiment and of the DMST prediction interfere, to become almost completely superimposed for the TSR of maximum Cp. Conversely, in the region of peak efficiency the 5-95-percentile uncertainty band remains above the curve computed without activating the dynamic stall model. This means that the application of the model is robust and quantitatively crucial, in the sense that even considering a very high uncertainty in its coefficients, the model is able to upgrade the predictive capability of the DMST code.

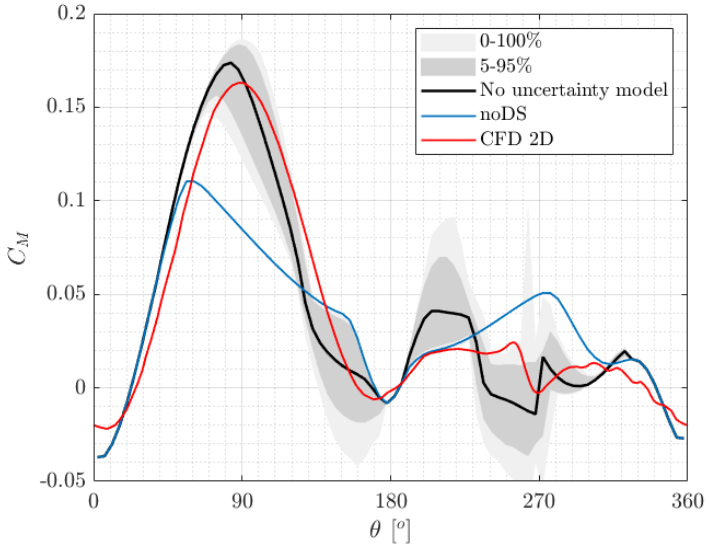

Figure 6. Power coefficient curve prediction with uncertainty bands against experiments.

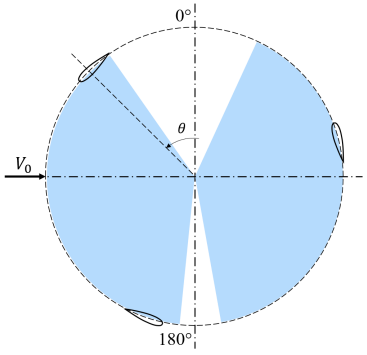

Figure 7. Torque exchanged by the rotor along the revolution for TSR = 2.4 with uncertainty bands against experiments.

An even more interesting result is found when considering the uncertainty in the torque coefficient distribution over a revolution for TSR = 2.4, reported in Figure 6, where the DMST prediction and its uncertainty bands are plotted alongside the calculation without dynamic stall and the CFD simulation result. As already commented, the dynamic-stall model improves the DMST-to-CFD comparison especially in the wide peak region comprised in the range $60^o \leq \theta \leq 120^o$. To better clarify the situation, Figure 7 reports a sketch of the revolution highlighting the fractions of the period in which the dynamic stall model is active for this specific TSR. It is interesting to note that exactly for $60^o \leq \theta \leq 120^o$ the dynamic stall model provides a crucial improvement in the prediction of the rotor torque against the CFD simulation, even though it also introduces a significant uncertainty. However, the systematic quantification performed indicates that the inherent model uncertainty is not sufficiently high to intersect the DMST prediction without dynamic stall.

High uncertainty is also found in the fraction of revolution corresponding to the leeward blade motion, i.e. in the range $135^o \leq \theta \leq 270^o$, that, as sketched in Figure 7, is also influenced by dynamic stall. In this region significant difference arise between the DMST and CFD trends, however such differences remain within the uncertainty band of the low-fidelity prediction. Moreover, the impact of the model in this region is, in general, of minor relevance for the overall rotor performance.

5. Conclusions

This paper has investigated the impact of the Strickland dynamic-stall model on the low-fidelity prediction of the performance of a small-scale H-shaped VAWT, at both deterministic and

stochastic level. To this end, an engineering simulation tool for VAWT performance prediction, based on the DMST method and supplemented with the most advanced high-order models, has been presented and validated against experiments over the entire operational curve of the turbine and against CFD simulations for one TSR close to peak efficiency. The DMST code was then routinely applied within an uncertainty quantification algorithm, based on the Monte-Carlo approach and supplemented by Kriging - Polynomial Chaos surrogate models, to evaluate the impact of the epistemic uncertainty of the dynamic stall model on the performance prediction.

The activation of the dynamic stall model was found to be crucial for improving the performance estimate of the code in the range of operative conditions close to peak efficiency. The comparison with CFD simulations has revealed that the model is particularly significant for an accurate prediction of the phase-resolved evolution of torque during the turbine revolution.

The systematic probabilistic analysis was performed by assuming large variability in the three empirical parameters appearing in the formulation. Results show that the uncertainty reflects in the power coefficient and in the torque exchanged by the blade during the revolution, especially in the upwind stroke of the blade motion. However, the uncertainty in the outputs remains relatively limited and, in the conditions around peak efficiency, it is comparable with that of the experiment.

As a final consideration, in the most relevant range of operation of the machine, for which the dynamic-stall model provides the largest benefit in the deterministic prediction of power coefficient, the predictions obtained without activating the dynamic-stall model do not fall within the 5-95-percentile uncertainty band of the full model. This indicates that the use of the dynamic-stall model is in general recommended, despite the inevitable uncertainty associated to the use of empirical correlations.

Future works will consider the application of the same UQ technique to the dynamic stall model of Leishmann and Beddoes, which is conceived with a completely different logic and makes use of an alternative set of empiric parameters. Moreover, the DMST code and the UQ tool will be applied to a small-scale Troposkien rotor for that geometry, operating conditions and a wide experimental database are available.

References

[1] Lam H F and Peng H Y 2016 *Renewable Energy* **90** pp 386–398
[2] Balduzzi F, Bianchini A, Ferrara G and Ferrari L 2016 *Energy* **97** pp 246–261
[3] Bianchini A, Balduzzi F, Ferrara G, Ferrari L, Persico G, Dossena V and Battisti L 2018 *Journal of Engineering for Gas Turbines and Power* **140**
[4] Franchina N, Persico G and Savini M 2019 *Renewable Energy* **136** pp 1170–89
[5] Paraschivoiu I 2002 *Wind Turbine Design: With Emphasis on Darrieus Concept* (Polytechnic International Press) p 438
[6] Bianchini A, Balduzzi F, Ferrara G, Persico G, Dossena V and Ferrari L 2019 *Journal of Engineering for Gas Turbines and Power* **141**
[7] Bangga G, Dessoky A, Lutz T and Kramer E 2019 *Energy* **182** pp 673–688
[8] Smith R 2013 *Uncertainty Quantification: Theory, Implementation, and Applications* vol 12 (SIAM)
[9] Martin J and TW S 2005 *AIAA Journal* **43** pp 853–863
[10] Crestaux T, Le Maitre O and Martinez J 2005 *Reliability Engineering & System Safety* **94** pp 1161–72
[11] Gormont R 1973 A mathematical model of unsteady aerodynamics and radial flow for application to helicopter rotors Tech. Rep. AD-767 240 Boeing Vertol Company
[12] Strickland J, Webster B and Nguyen T 1980 A vortex model of the darrieus turbine: an analytical and experimental study Tech. Rep. SAND 79-7058 SANDIA
[13] Leishman J and Beddoes T 1986 A generalized model for airfoil unsteady aerodynamic behaviour and dynamic stall using the indical method *42nd Annual Forum of the American Helicopter Society* (Washington D. C., USA)
[14] Sheng W, Galbraith R A M and Coton F N 2008 *Journal of Solar Energy Engineering* **130**
[15] Battisti L, Persico G, Dossena V, Paradiso B, Raciti Castelli M, Brighenti A and Benini E 2018 *Renewable Energy* **125** pp 425–444

[16] Battisti L Raciti Castelli M, Brighenti A, Dossena V and Persico G 2018 *Journal of Physics: Conf. Series* **1037**
[17] Dossena V, Persico G, Paradiso B, Battisti L, Dell'Anna S, Benini E and Brighenti A 2015 *ASME Journal of Energy Resources Technology* **137**
[18] Bianchini A, Balduzzi F, Rainbird J, Peiro J, Graham J, Ferrara G and Ferrari L 2016 *Journal of Engineering for Gas Turbines and Power* **138**
[19] Viterna L A and Janetzke D 1982 Theoretical and experimental power from large horizontal-axis wind turbines Tech. Rep. NASA-TM-82944 NASA Lewis Research Center, Cleveland, OH
[20] Battisti L 2011 *Gli impianti motori eolici* (Green Place Energies)
[21] Buhl M L 2005 A new empirical relationship between thrust coefficient and induction factor for the turbulent windmill states Technical Report NREL TP- 500-36834 National Renewable Energy Laboratory
[22] Goude A 2012 *Fluid Mechanics of Vertical Axis Turbines - Simulations and Model Development* Ph.D. thesis Uppsala Universitet Sweden
[23] Balduzzi F, Bianchini A, Ferrara G and Ferrari L 2016 *Energy* **97** pp 246–261
[24] Peretti L 2017 Investigation on several turbulence models for a two-dimensional simulation of a H-type Darrieus wind turbine. Master Thesis, Politecnico di Milano
[25] Marelli S and Sudret B UQLab - The Framework for Uncertainty Quantification Tech. rep. ETH Zurich